



Detection of human κ -opioid antibody using microresonators with integrated optical readout

Erman Timurdogan^a, Natali Ozber^b, Sezin Nargul^b, Serhat Yavuz^c, M. Salih Kilic^c, I. Halil Kavakli^b, Hakan Urey^a, B. Erdem Alaca^{c,*}

^a Department of Electrical and Electronics Engineering, Koc University, Rumeli Feneri Yolu, 34450 Sariyer, Istanbul, Turkey

^b Department of Chemical and Biological Engineering, Koc University, Rumeli Feneri Yolu, 34450 Sariyer, Istanbul, Turkey

^c Department of Mechanical Engineering, Koc University, Rumeli Feneri Yolu, 34450 Sariyer, Istanbul, Turkey

ARTICLE INFO

Article history:

Received 21 February 2010

Received in revised form 30 May 2010

Accepted 7 June 2010

Available online 11 June 2010

Keywords:

Microcantilever immunosensor

Resonator

Electromagnetic actuation

Diffraction grating interferometry

Integrated readout

Protein–antibody interaction

ABSTRACT

Label-free detection of the interaction between hexahistidine-tagged human κ -opioid receptor membrane protein and anti-His antibody is demonstrated in liquid by an optical microelectromechanical system utilizing electromagnetically actuated microresonators. Shift in resonance frequency due to accretion of mass on the sensitive surface of microresonators is monitored via an integrated optical readout. A frequency resolution of 2 Hz is obtained. Together with a sensitivity of 7 ppm/(ng/ml) this leads to a minimum detectable antibody concentration of 5.7 ng/ml for a 50-kHz device. The measurement principle is shown to impart immunity to environmental noise, facilitate operation in liquid media and bring about the prospect for further miniaturization of actuator and readout leading to a portable biochemical sensor.

© 2010 Elsevier B.V. All rights reserved.

1. Introduction

Microcantilever arrays find various applications as the transducer element in label-free biological sensing. Some of the advantages associated with the use of microcantilevers include lower detection limits thanks to miniaturization, the ability of shape optimization of cantilevers or selective placement of functionalized regions on a cantilever, cost reduction due to the ability of batch processing and the possibility of working on large arrays, which can be integrated with electronics. The extent of these advantages is closely related to the capabilities of utilized microfabrication techniques (Hierlemann et al., 2003). Cantilevers are used both in static and in dynamic modes. In each case, cantilever surface is functionalized with a selective layer of biomolecules that interact with target molecules. A historical background on the studies of mechanical phenomena in a changing chemical environment can be found in Lavrik et al. (2004). In the static mode this interaction leads to surface stress generation and hence, bending of the cantilever. The amount of this bending serves as a quantitative indication of the magnitude of the surface stress and can be measured through various readout schemes including optical and piezoresistive. In addition to surface stresses, swelling of a surface coating in a bima-

terial cantilever also leads to bending in a similar fashion (Lavrik et al., 2004; Ziegler, 2004). In the dynamic mode, the shift in resonance frequency as a result of mass accretion on cantilever surface is monitored. Any mass deposition on the surface leads to a reduction of resonance frequency, although non-gravimetric effects can also become significant (Lucklum and Hauptmann, 2006).

In the dynamic mode, quality factor, Q factor, is a measure of energy loss per cycle and hence, it serves as an important indication of damping in the system. In frequency domain, it is defined as the ratio of the resonance frequency, f_0 , to the bandwidth where the amplitude of the signal drops to $1/\sqrt{2}$ of the amplitude at resonance frequency. The vibration amplitude of a cantilever with a high Q factor drops more rapidly when diverging from the resonance frequency compared with that of a low- Q system. Hence, a high Q factor would decrease the minimum detectable mass (Tamayo, 2005). Various recent studies demonstrated higher quality factors with higher order modes (Verbridge et al., 2006; Ekinci and Roukes, 2005). Liquid operation in dynamic mode poses problems in this respect since it is accompanied by the damping of the out-of-plane vibration of cantilever resonators. The result is a reduction in Q factor. Therefore static mode operation has been traditionally utilized in biological measurements in liquid media with great success. Some of the reported works include the sensing of non-amplified RNA in total RNA within a cell with a detection limit of 10 pM (Zhang et al., 2006) and the detection of peptides with a detection limit on the order of 1 nM (Backmann et al., 2005). Dynamic operation

* Corresponding author. Tel.: +90 212 338 1727; fax: +90 212 338 1548.

E-mail address: éalaca@ku.edu.tr (B.E. Alaca).

in liquid media usually necessitates Q factor enhancement using an amplifying feedback loop (Anczykowski et al., 1998; Li et al., 2003; Konduri et al., 2009). Successful applications of the resonant mode include the measurement of antigen–antibody interactions (Hwang et al., 2004), the detection of pathogen spores (Campbell and Mutharasan, 2007) and DNA hybridization (Ramos et al., 2009).

In this study, a microcantilever array is used for the detection of biological species in dynamic mode inside the buffer solution with enhanced electromagnetic actuation. T-shaped Ni–Au double-layered cantilevers are fabricated with diffraction gratings at their tips facilitating the utilization of a simple optical readout technique (Ozturk et al., 2008). The diffraction grating integrated on the cantilever serves as a moving surface, whereas the stationary Si substrate, on which devices are fabricated, is a measurement reference. Intensity modulation in a diffraction order can then be monitored with a photodiode and cantilever's vibration frequency can thus be measured. Cantilevers are characterized in terms of resonance characteristics. Their potential as a bio-selective mass sensor is demonstrated with simulant antibodies of narcotic molecules. Their simple architecture with the possibility of extension to a vast array combined with liquid operation and immunity against environmental noise as demonstrated in this work are provided as promising aspects of the proposed transducer to be used in a low-cost, label-free and portable biosensor with parallel readout. Some of the advantages associated with the proposed technology include: (1) There are no electrical connections on the MEMS (micro electromechanical systems) sensor, allowing for a completely disposable sensor. (2) Optical detection method is suitable for multiplexed operation. (3) Operation both in air and in liquid is allowed. (4) The sensor is more robust compared to Doppler vibrometry and other optical readout techniques. (5) Readout is not affected by the refractive index variations due to dynamic mode operation that monitors the frequency instead of deflection.

Detection of narcotics is necessary to evaluate drug exposure in several fields, such as workplace drug testing, drug-facilitated crimes, pre-natal exposure to drugs, doping control, and therapeutic drug monitoring of pharmaceuticals. Currently, detection of drugs from biological fluid samples (blood and urine) are performed using various methods including liquid chromatography with tandem mass spectrometry, ELISA, HPLC and gas chromatography. These platforms are expensive and require technical expertise for operation. Therefore, development of an easy-to-use, label-free, portable and cost-effective biosensor would especially be useful for the detection of narcotics. To the best of our knowledge, this study presents the first effort to develop such narcotics detection technology using human opioid receptors (Lachenmeier et al., 2010).

In the following, design and fabrication of cantilevers will be explained followed by a description of the measurement setup. Measurements will be compared against those obtained with a commercial Doppler vibrometer. Higher order modes obtained in air and liquid will be characterized. Functionalization with hexahistidine-tagged human κ -opioid receptor (hKOR) membrane protein and measurement protocols will be described. Finally, the results of the detection of interaction between His tagged hKOR and anti-His antibody will be presented.

2. Materials and methods

2.1. Design and fabrication of cantilever chips

The resonance frequency of the first mode of a cantilever is defined as:

$$f_0 = \frac{1}{2\pi} \sqrt{\frac{k}{m^*}}, \quad (1)$$

where k is the bending stiffness and m^* is the effective mass of the cantilever beam and can be expressed as $m^* = n(\rho wlt)$, where n is a geometry-dependent constant ($1 > n > 0$), ρ is the density and w , l and t are the width, length and thickness of the cantilever beam, respectively. For one-end-fixed cantilevers n is equal to 0.24 (Park et al., 2007; Varshney et al., 2008).

The amount of accreted mass, Δm , responsible for a shift in the resonance frequency from f_0 to f'_0 is given by Ono et al. (2003):

$$\Delta m = \frac{k}{4\pi^2} \left(\frac{1}{f'^2_0} - \frac{1}{f^2_0} \right), \quad (2)$$

where the stiffness of the cantilever is assumed to remain constant.

Quantification of adsorbed mass in liquid becomes especially challenging due to density and viscosity effects. Therefore in biosensing applications it is more practical to work in terms of concentration, C , rather than absolute mass. In this case the sensitivity, S , can be expressed as:

$$S = \frac{\partial f_0}{\partial C}. \quad (3)$$

As the resonance frequency increases and mass of the resonator decreases, transducer sensitivity will increase. S also determines the detection limit, i.e. the minimum detectable concentration, C_{\min} , of the device as shown in Eq. (4).

$$C_{\min} = S^{-1} \delta f_0, \quad (4)$$

where δf_0 is the noise in detecting the resonance frequency (Fan et al., 2008).

Fabrication of cantilever chips follows an earlier work reported in Ozturk et al. (2008). Ni cantilevers used in the experiments are fabricated with a single-mask photolithographic process. A 20 nm/100 nm Cr/Au layer is deposited on a 4" (100) single crystalline silicon wafer via RF sputtering. Au layer serves as the seed layer for subsequent Ni electroplating and a platform for biological functionalization thereafter. Au surface is patterned with UV photolithography using 1.4- μm thick AZ 5214[®] photoresist (PR). PR layer is used as a mold to be filled via electroplating of Ni. The cantilevers are designed to include a platform at their free ends for the integration of optical (interferometric) readout using diffraction grating. The inset in Fig. 1 illustrates a series of four cantilevers with integrated diffraction gratings.

After photolithography the wafer is sliced into dice and the cantilever beam structures are obtained by electrodeposition of Ni on each die. The reason for choosing Ni is its high resistance to oxidative and corrosive agents, and its suitability for remote magnetic actuation, which altogether imply adequate reliability for biosensing applications. For electrodeposition, a nickel sulphamate bath that is composed of 600 g/l nickel sulphamate ($\text{Ni}(\text{SO}_3\text{NH}_2)_2 \cdot 4\text{H}_2\text{O}$), 10 g/l nickel chloride ($\text{NiCl}_2 \cdot 6\text{H}_2\text{O}$) and 40 g/l boric acid (H_3BO_3) is used. Adjusting current density, temperature and duration of the deposition, thickness and surface roughness of cantilevers can be controlled. During electroplating, a current density of about 40 mA/cm² is used. To achieve a homogenous and reflective Ni surface, electrical contact is established along four edges of a die and the deposition solution is continuously stirred. To achieve highest Ni modulus for highest resonance frequency, deposition temperature is set to around 45 °C (Luo et al., 2004).

After cantilevers are obtained by electroplating, PR is stripped using AZ 100[®] remover and exposed films of Au and Cr are removed consecutively by wet etching. Au is time-etched to preserve the Au layer underneath cantilevers. The presence of such a layer is later verified by scanning electron microscopy. Cantilevers are released by anisotropic wet etching of Si layer with 35% KOH solution at 65 °C to optimize the roughness of Si surface and prevent stiction of the cantilevers (Noor et al., 2002). An average surface roughness of

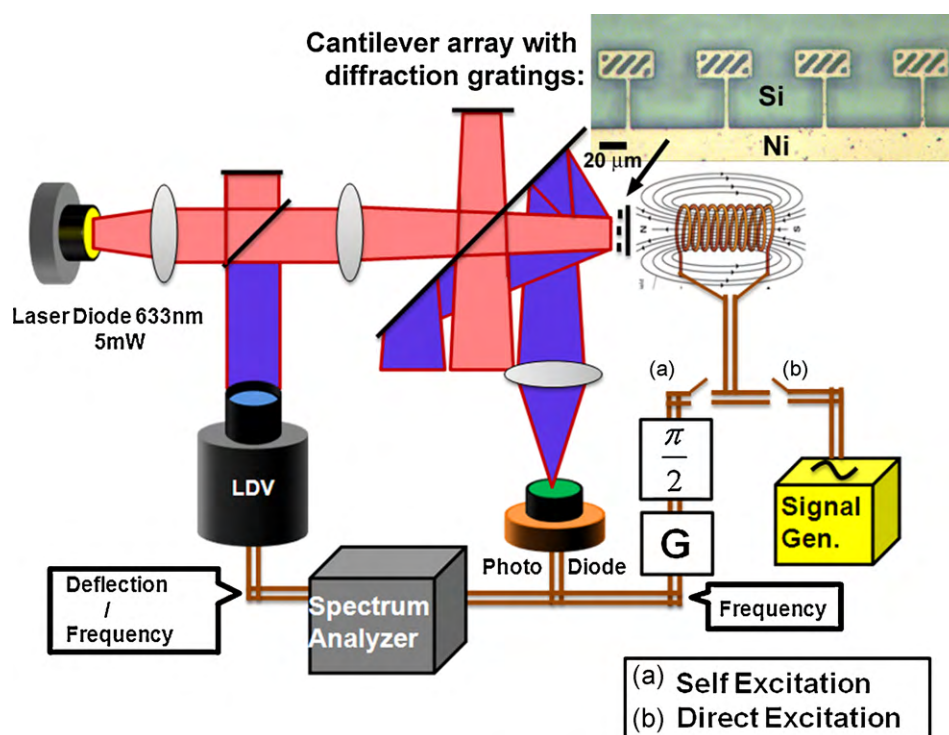


Fig. 1. Schematic representation of the measurement setup with self-excitation and direct excitation options. The inset shows an array of microcantilevers with diffraction gratings at their tips.

3–10 nm is measured for Si surface by surface profilometry. Etching is carried out to a depth of 10–20 μm to avoid squeeze film damping effects (Bao and Yang, 2007). After Si etch, the Cr layer underneath the cantilevers is removed completely by wet etching, leaving the Au layer exposed for later biological functionalization. The inset in Fig. 1 shows a complete array of 3-μm wide microcantilevers with a length of 40 μm.

2.2. Measurement principle and setup

Diffraction grating shown in Fig. 1 plays a major role in measurements. An interference pattern is formed by two laser beams (He–Ne laser with ~633 nm wavelength), one reflecting from resonator surface and the other one from the bottom Si substrate. This leads to an intensity modulation on the photodiode in response to the deflection of Ni cantilever with respect to the Si reference surface.

The intensity of diffraction orders changes periodically with the gap between the cantilever and the substrate with a period of half the wavelength of the incident laser on the cantilevers. Utilizing the intensity modulation of the diffraction orders, deflection amplitude (or phase) of the cantilever can be monitored (Isikman et al., 2007; Ferhanoglu et al., 2007; Hall and Degertekin, 2002). The resonance frequency can then be obtained as the frequency where the maximum peak-to-peak voltage is observed. In the case of phase measurements, this corresponds to the frequency at which there is a 90° phase difference with respect to the actuation signal.

Measurement setup utilized in this work is shown in Fig. 1. Actuation can be carried out with two different methods: closed-loop self-oscillation and direct excitation. For biosensing study, closed-loop self-oscillation is used (switch a in Fig. 1). For MEMS characterization direct excitation method is used where an external sinusoidal AC signal is applied to electrocoil (switch b in Fig. 1). Electromagnetic actuation is superior to many conventional approaches since it enables operation in liquid media and makes the sensor array disposable and remote from optic and electronic equipment.

For the biosensing experiments self-oscillation method is used (switch a in Fig. 1) and the sample is immersed in fluidic environment using a custom-made 1 ml flowcell. SNR is higher and multiplexing for multi-analyte screening is possible as it does not require separate signal generators for each MEMS cantilever. In order to trigger oscillations, Brownian deflection of the cantilever, obtained from the photodiode, is multiplied with a gain of G and $\pi/2$ phase shifted and used as a feedback electromagnetic force to the cantilevers. When the uncorrelated noise component is considered negligible which is an advantage of utilizing optical interference principle and the Brownian deflection is assumed sinusoidal, equation of motion of the overall system can be expressed as follows:

$$e^{j\pi}x + \frac{b}{m}e^{j(\pi/2)}x + \frac{k}{m}x = Ge^{j(\pi/2)}x \quad (5)$$

where x is the Brownian deflection, m is the effective mass of the cantilever, b is the total damping and k is the spring constant of the cantilever. Gain is adjusted just above a critical value of $G = b/m$ and oscillations rise rapidly and saturate at a stable oscillation frequency. This is equivalent to tuning of hydrodynamic damping to trigger oscillations and called as self-excitation. (Tamayo et al., 2007; Konduri et al., 2009) This technique increases SNR and it is suitable for multi-analyte screening since multiple cantilevers can be self-excited with a single coil and one $\pi/2$ phase shifter circuitry. In this work, self-excitation is utilized for particularly sensing His tagged hKOR protein in liquid to eliminate experimental errors caused by temperature, humidity change and wetting of the cantilevers with the compromise of lower quality factor and SNR (Singamaneni et al., 2008).

2.3. Measurement of biological samples

In this study, His tagged hKOR membrane protein, which can bind to narcotic molecules, is immobilized on the Au surface underneath Ni cantilevers. Instead of actual ligands, anti-His antibody proteins are used in all of the experiments as the drug simulant. The

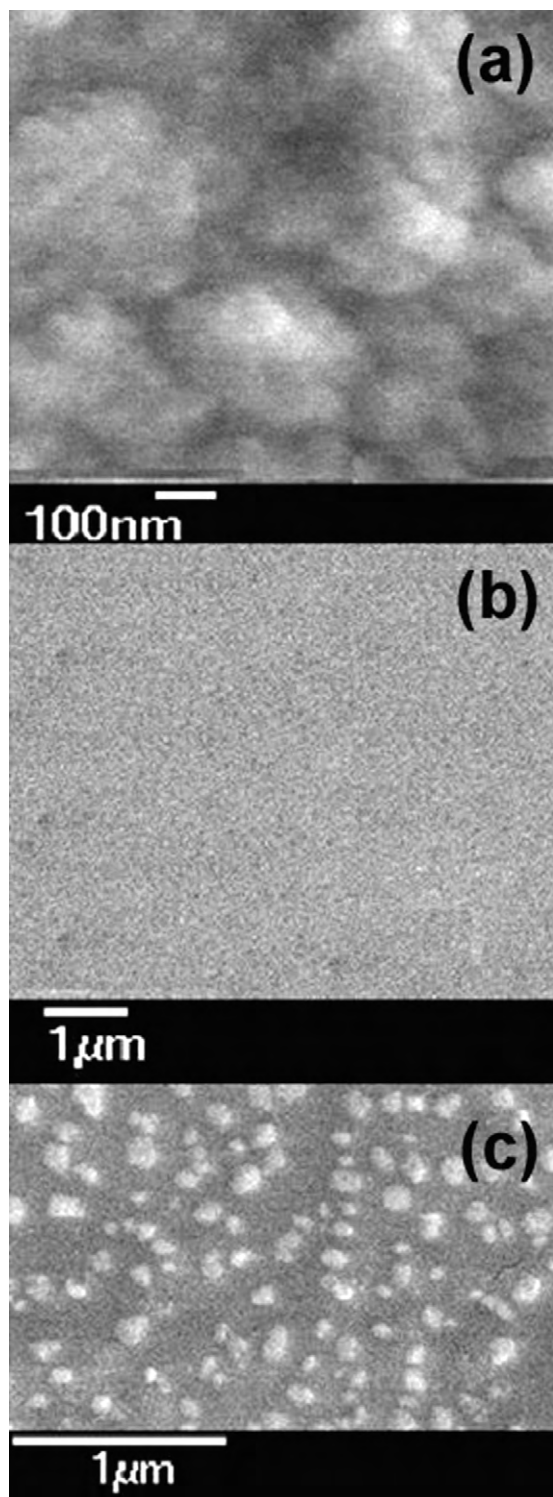


Fig. 2. Scanning electron micrographs of (a) Au, (b) Au and hKOR, (c) Au, hKOR and anti-His antibody.

shifts in resonance frequencies due to the biochemical accretion of protein molecules on cantilevers are observed for two separate processes: (1) binding of His tagged hKOR molecules to the cantilevers up to saturation point and (2) binding of anti-His antibody molecules to the receptor molecules with different concentrations. All measurements are taken at 23–24.5 °C temperature window within a 1-ml flowcell.

In order to eliminate various background effects including fabrication variations and ensure perfect binding on the sensor array, all biosensing measurements are made in liquid inside a flowcell with two sensor arrays. Same buffer solution (PBS) is used in all experiments, and cantilevers are not exposed to air. Sensor arrays are placed separately inside the flowcell in a clean room to avoid dust particles and oxidation on the cantilever surface. First microcantilever sensor array is composed of 39 cantilevers with 3 different sets of 13 cantilevers corresponding to cantilever lengths of 25, 50 and 75 μm (resonance frequency range: 25–90 kHz). Grating platform has dimensions of 18 μm by 35 μm. Cantilever thickness and width are kept constant at 1.1 and 5.0 μm, respectively. Resonance frequencies in buffer are taken as initial measurements. Then, the sensor array is functionalized with a linker Dithiobis (succinimidyl propionate) (DSP), which will bind both protein through amine group and gold through the sulphur group. Then cantilever surfaces are saturated with hKOR with the method that will be discussed in Section 2.4. Finally, the flowcell is filled with different anti-His antibody concentrations (from 80 ng/ml to 2 μg/ml) to obtain the sensitivity curve.

Sensitivity to viscosity and other background effects is investigated with the second microcantilever sensor array, which serves as the reference chip (in the presence of only anti-His antibody). This array is composed of 21 cantilevers with 3 different sets of 7 cantilevers corresponding to cantilever lengths of 20, 40 and 60 μm (resonance frequency range: 20–50 kHz). Grating platform has identical dimensions of 18 μm by 35 μm. Cantilever thickness and width are kept constant at 1.1 and 4.0 μm, respectively. Experimental procedure is same as the one employed with the first sensor array except for the DSP stage. In the absence of DSP reference resonance frequencies are observed as almost constant throughout the measurements for this array.

2.4. Biological functionalization

2.4.1. Cloning hKOR gene into an expression vector

The cDNA of human κ-opioid receptor (hKOR) is cloned into pMAL-c2x as in Ozber et al. (2008). The His-tag sequence is placed in the hKOR by PCR amplification under the condition of 95 °C for 30 s, 55 °C for 30 s and 72 °C for 2 min, for 30 cycles. Amplified hKOR is cloned to downstream of malE gene, which encodes maltose-binding protein (MBP), in the pMAL-c2x.

2.4.2. Expression and purification of hKOR

The recombinant hKOR is expressed in *Escherichia coli* DH5α cells and purified through Ni-NTA affinity chromatography as described in Ozber et al. (2008) with several modifications. Briefly, *E. coli* containing hKOR are grown at 37 °C to an OD₆₀₀ of 0.5–0.8 with vigorous shaking. The expression of hKOR is induced with 0.5 mM IPTG (isopropyl-1-thio-β-D-galactopyranoside) for 3 h. Cells are then harvested and disrupted in lysis buffer (10 mM Tris-HCl, pH 8.0, 1 mg/ml lysozyme). Crude cell extracts are obtained by centrifugation at 10,000 × g for 45 min at 4 °C. Following solubilization of membrane in solubilization buffer (100 mM NaH₂PO₄, pH 8.0, 10 mM Tris-HCl, pH 8.0, 20 mM β-mercaptoethanol, and 0.1% of SDS (sodium dodecyl sulphate)), solubilized proteins are obtained by centrifugation at 20,000 × g for 1 h and loaded on a Ni-NTA agarose resin pre-equilibrated with solubilization buffer. The eluted proteins are dialyzed against functionalization buffer (100 mM NaH₂PO₄, pH 8.0, and 10 mM Tris-HCl, pH 8.0.) At the time of functionalization, hKOR is freshly purified.

2.4.3. SDS-PAGE and western blotting

First, proteins are subjected to 10% SDS-PAGE Bio-Rad Mini-PROTEAN III at 150 V for 1.5 h. Then, gels are transferred to

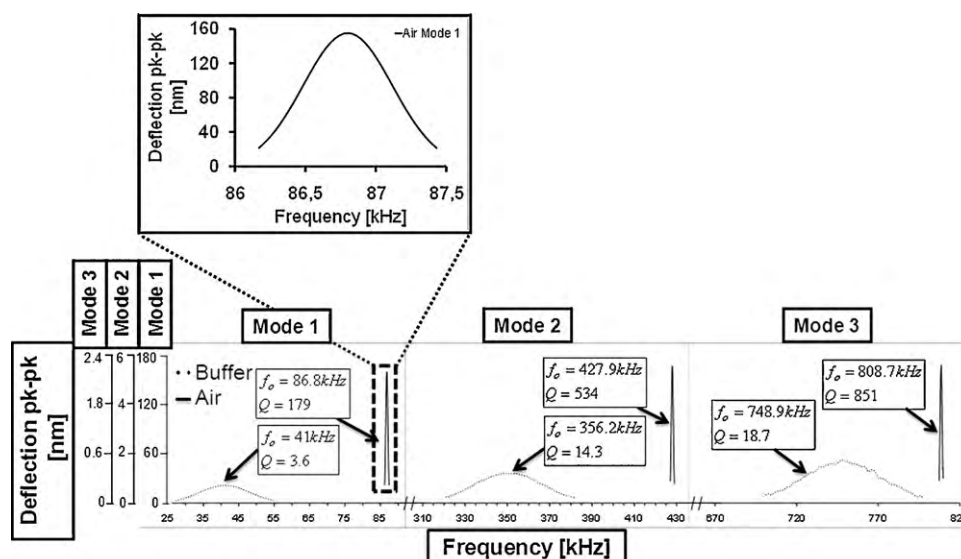


Fig. 3. Comparison of the first three bending modes of a sample cantilever in air and in liquid.

polyvinylidene difluoride membrane (Biotrace PVDF, Pall Corporation, FL, USA) with a Mini-Trans-Blot electrophoretic transfer cell (Bio-Rad) at 90 V for 1 h. After pre-blocking with 5% BSA dissolved in Tris-buffered saline (TBS), the membrane is incubated with anti-His (50 μg in 0.05% Tween 20/TBS) (Santa Cruz) for 1 h at room temperature. After a series of washes the membrane is subsequently incubated with AP-conjugated secondary anti-mouse IgG antibody (100 ng in 0.05% Tween 20/TBS) (S41176, Sigma) for 1 h. Proteins are visualized by NBT/BCIP detection system (Roche).

2.4.4. Functionalization of the cantilevers

Chips are cleaned through a standard RCA-1 procedure and placed in a flowcell, where all measurements and processes are carried out. Immobilization of purified hKOR to the cantilevers is achieved through DSP linker on gold surface as follows: First, surface is treated with 1 mM of DSP for 30 min at room temperature (Ozber et al., 2008). Then gold surface is washed with dimethyl sulphoxide (DMSO) and PBS buffer to remove unbound DSP linker. Then 1 ml (containing 1 mg of protein) of hKOR protein in PBS is introduced into the flowcell and incubated for 1 h at room temperature. At this point measurement is taken directly in flowcell in liquid. Proteins are then removed by replacing with PBS and chips are washed three times. Binding experiments are carried out at six different antibody concentrations from 80 ng/ml to 2 μg /ml. Starting from the lowest concentration antibody for each concentration is introduced into the flowcell and binding of antibody to hKOR

is measured. Each time antibodies are incubated for 1 h at room temperature and chips are rinsed with PBS after each treatment.

2.4.5. Scanning electron microscopy

Scanning electron microscopy (SEM) analysis is performed using a JSM-5600LV microscope (JEOL Ltd., Japan) with 20 kV accelerating voltage to characterize the morphology of (i) gold surface, (ii) gold surface covered with hKOR and (iii) gold surface covered with hKOR with its antibody.

3. Results and discussion

Western blot analysis of the purified hKOR shows an apparent molecular weight of 85 kDa with fusion protein MBP (~ 40 kDa). The receptor remains intact and stable under this purification system since there is no degradation product observed (data are not shown).

Purified hKOR is attached to the Au surface through a DSP linker. Then SEM is performed to see first the functionalization of Au surface with hKOR and then the attachment of hKOR to its antibody. Fig. 2a shows a typical Au surface prior to functionalization. After functionalization, only an energy-dispersive X-ray spectroscopy (EDS) analysis can demonstrate a uniform distribution of hKOR proteins on the Au surface, where visually there is no difference (Fig. 2b). After the exposure to His antibody, surface morphology changes drastically (Fig. 2c).

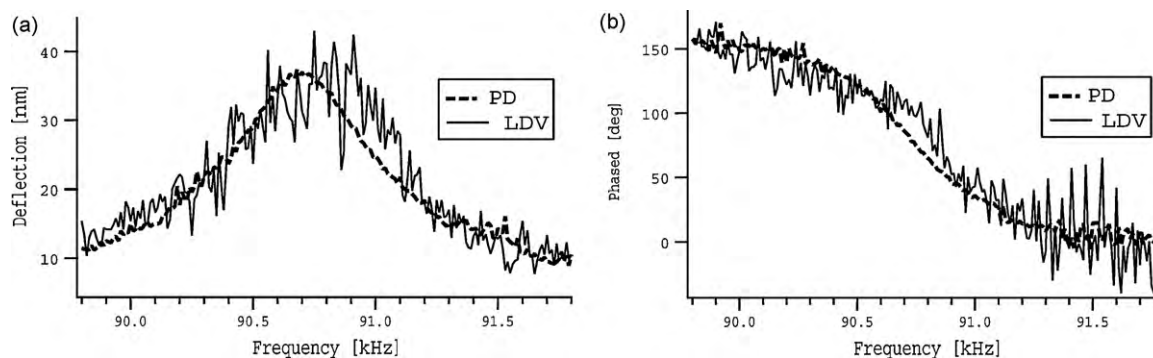


Fig. 4. Comparison of LDV and PD measurements for a cantilever of dimensions $w = 12 \mu\text{m}$ and $L = 60 \mu\text{m}$, in the presence of the same mechanical noise source: (a) amplitude plot and (b) phase plot of the frequency responses of PD and LDV measurements.

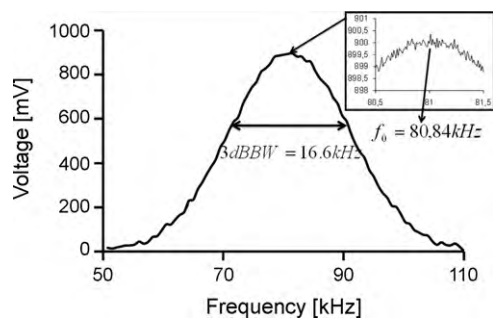


Fig. 5. A sample frequency sweep curve in buffer.

Meanwhile operation in liquid with direct excitation is demonstrated with direct excitation switch is closed (switch b in Fig. 1). In Fig. 3 measurements taken in DMSO for the first three bending modes of a sample cantilever with dimensions $w = 5 \mu\text{m}$ and $L = 50 \mu\text{m}$ are shown in comparison with the measurements in air. The resonance frequency curves of the cantilevers are obtained by measuring the peak-to-peak deflection of the cantilevers over a bandwidth of frequencies with the help of an oscilloscope and a GPIB-interfaced PC and quantified by a Lorentzian fit function. Quality factor is observed to increase with increasing mode number since less amount of liquid is moved by the cantilever (Ghatkesar et al., 2008).

Optical readout method developed in this work is robust and suitable for portable devices. To prove this point, an experiment is performed to compare the simple single photodetector measurement results with laser Doppler vibrometry (LDV). LDV measurement typically requires averaging and floating of the optical table for measuring nanometric deflections. Data of a similar comparison in Ozturk et al. (2008) were obtained using such an averaging procedure. Fig. 4 presents a comparison of simple photodiode (PD) measurement and LDV data in the presence of mechanical noise. No averaging was carried out while obtaining these data. Hence, simple PD readout proves more robust and suitable for portable sensing and field applications compared to a commercial LDV, and similarly, to knife-edge based methods used in AFM and other sensors.

Another important parameter is the frequency resolution. Although SNR of the readout signal and quality factor of the cantilever decrease in liquid, it is possible to measure the resonance peak with a spectrum analyzer with high precision. Spectrum analyzer utilized in measurements has a frequency resolution of 2 Hz. At this frequency resonance frequency sweeps are recorded for up to 60 s, and no deviation in the central frequency is observed over this time window. Since the peak remains stable, it is concluded that we have an accuracy of 2 Hz. In Fig. 5, the broad resonance frequency peak with 3 dB bandwidth of 16 kHz is located and the peak location is zoomed manually to a 1 kHz window with 2 Hz precision or bandwidth, then automatic peak finding capability of the spectrum analyzer is utilized to determine the peak location accurately. With multiple cantilever measurements and averaging, SNR can further be increased leading to better frequency resolution. Further analysis and characterization is necessary at this point.

After the characterization of the transducer and SEM observations, measurements on actual biological system are performed in liquid. Resulting frequency shifts are shown in Fig. 6 both for the reference chip (only antibody in buffer) and the protein chip (hKOR+antibody). The linear range in the sensor response (up to a concentration of about 400 ng/ml) exhibits a sensitivity of 7 ppm/(ng/ml). For a 50-kHz device, this sensitivity translates into 0.35 Hz/(ng/ml). With a frequency resolution of 2 Hz of the present instrumentation, a minimum detection limit of 5.7 ng/ml

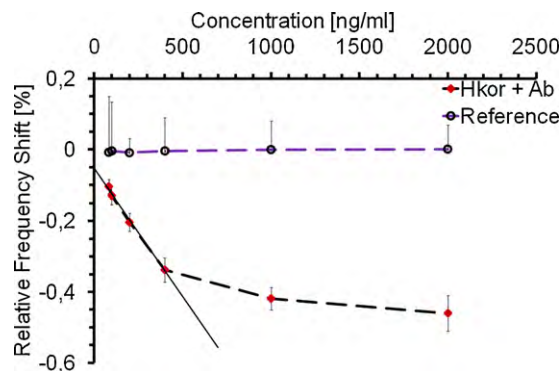


Fig. 6. Sensitivity curves of protein and reference chips, where normalized frequency shift (in %) is plotted against antibody concentration. Protein chip exhibits a sensitivity of 7 ppm/(ng/ml) over its linear range (up to about 400 ng/ml).

is obtained. It should be emphasized at this point that this limit is obtained by extrapolation using frequency resolution in accordance with Eq. 4, and the minimum concentration used in experiments was 80 ng/ml. The detection limit can further be improved by multiple cantilever measurements and averaging as explained earlier. It is also clear in Fig. 6 that anti-His antibody is detectable up to 1.1 $\mu\text{g/ml}$, beyond which sensor response would saturate. On the other hand, no sensitivity is observed on the reference chip. To avoid ambiguity on Fig. 6, error bars of reference measurements are indicated only by positive relative shifts.

This method is also insensitive to changes in the refractive index as opposed to many optical methods including cantilever sensors operated in static mode. This is especially critical for biosensing operations, where liquid operation and multi-analyte screening are required. Immunity against variations in refractive index is thanks to the fact that the resonant frequency does not change with refractive index. Although temperature variations in experiments are kept small, a full characterization of temperature dependence is also under study. For sensing purposes, taking reference measurements at every step using identical, non-functionalized cantilevers can be used to eliminate temperature sensitivity.

4. Conclusions

Specific detection of a biological interaction between the hKOR protein and drug simulant antibody (anti-His) is demonstrated using resonant mass sensing method with electromagnetically actuated and diffraction grating integrated Ni microcantilevers. The mechanical noise immunity of the readout system is compared to that of a commercially available LDV system, demonstrating a more robust response to the same noise source. In addition, operation with higher order modes is carried out both in air and in buffer in order to demonstrate suitability for measurements in aqueous solutions with higher sensitivities.

The sensor response is found to be linear up to a concentration of 400 ng/ml with a sensitivity of 7 ppm/(ng/ml) leading to a minimum detection limit of 5.7 ng/ml for a 50-kHz resonator. With multiple cantilever measurements and averaging, SNR in frequency measurements can be increased leading to an improvement of frequency resolution. The range of concentrations and the detection limit are comparable to other immunosensing studies utilizing microgravimetry reviewed in (Leca-Bouvier and Blum, 2005).

These observations indicate a potential for the development of a low-cost and portable mass sensor for real-time monitoring of biochemical reactions. It can be integrated with a low-cost feedback circuitry, which also enables a parallel readout of an array of cantilevers for a high throughput bio-selective detection. The measurements can be carried out in aqueous medium for faster and

more accurate results, and in vacuum, to observe the actual sensitivity limits of the microcantilevers and the measurement setup. In addition, the quality factor can be enhanced by employing higher order modes.

Furthermore, for the first time a membrane protein (human κ -opioid membrane protein) which is successfully immobilized on cantilever is detected with its antibody, and a specific detection of interaction between hKOR and anti-His antibody is demonstrated. Broad range of drugs can be detected by immobilization of other types of receptors. It may also be possible to use such an approach to detect narcotics from the biological samples.

Acknowledgements

Authors acknowledge support by TUBITAK under Grant No. 105E148 and 109E222. The work of B. E. Alaca, H. Urey and I. H. Kavakli was supported by a TUBA-GEBIP Distinguished Young Scientist award.

References

- Anczykowski, B., Cleveland, J.P., et al., 1998. *Appl. Phys. A* 66, S885–S889.
- Backmann, N., Zahnd, C., et al., 2005. *Proc. Natl. Acad. Sci. U.S.A* 102, 14587–14592.
- Bao, M., Yang, H., 2007. *Sens. Actuators A* 136, 3–27.
- Campbell, G.A., Mutharasan, R., 2007. *Anal. Chem.* 79, 1145–1152.
- Ekinci, K.L., Roukes, M.L., 2005. *Rev. Sci. Instrum.* 76, 061101.
- Fan, X.D., White, I.M., et al., 2008. *Anal. Chim. Acta* 620, 8–26.
- Ferhanoglu, O., Toy, M.F., et al., 2007. *IEEE Photonics Technol. Lett.* 19, 1895–1897.
- Ghatkesar, M.K., Braun, T., et al., 2008. *Appl. Phys. Lett.* 92, 043106.
- Hall, N.A., Degertekin, F.L., 2002. *Appl. Phys. Lett.* 80, 3859–3861.
- Hierlemann, A., Brand, O., et al., 2003. *Proc. IEEE* 91, 839–863.
- Hwang, K.S., Lee, J.H., et al., 2004. *Lab Chip* 4, 547–552.
- Isikman, S.O., Ergeneman, O., et al., 2007. *IEEE J. Sel. Top. Quantum Electron.* 12, 283–289.
- Konduri, S., Patra, S., et al., 2009. *Proc. Int. Conf. MEMS, OM–01*.
- Lavrik, N.V., Sepaniak, M.J., et al., 2004. *Rev. Sci. Instrum.* 75, 2229–2253.
- Lachenmeier, D.W., Sproll, C., et al., 2010. *Ther. Drug. Monit.* 32, 11–18.
- Leca-Bouvier, B., Blum, L.J., 2005. *Anal. Lett.* 38, 1491–1517.
- Li, Y., Vancura, C., et al., 2003. *Proc. IEEE Sens.* 2, 809–813.
- Lucklum, R., Hauptmann, P., 2006. *Anal. Bioanal. Chem.* 384, 667–682.
- Luo, K.K., Flewitt, A.J., et al., 2004. *Mater. Sci. Lett.* 58, 2306–2309.
- Noor, M.M., Bais, B., et al., 2002. *Proc. IEEE Int. Conf. Semicond. Electron.*, 524–528.
- Ono, T., Li, X.X., et al., 2003. *Rev. Sci. Instrum.* 74, 1240–1243.
- Ozber, N., Ozturk, A., et al., 2008. *Proc. IASTED Int. Conf. Nanotechnol. Appl.*, 33–36.
- Ozturk, A., Ocakli, H.I., et al., 2008. *IEEE Photonics Technol. Lett.* 20, 1905–1907.
- Park, K.K., Lee, H.J., et al., 2007. *Appl. Phys. Lett.* 91, 094102.
- Ramos, D., Arroyo-Hernandez, M., et al., 2009. *Anal. Chem.* 81, 2274–2279.
- Singamaneni, S., et al., 2008. *Adv. Mater.* 20, 653–680.
- Tamayo, J., 2005. *J. Appl. Phys.* 97, 044903.
- Tamayo, J., et al., 2007. *Phys. Rev. B* 76, 180201.
- Varshney, M., Waggoner, P.S., et al., 2008. *Anal. Chem.* 80, 2141–2148.
- Verbridge, S.S., PArpia, J.M., et al., 2006. *J. Appl. Phys.* 99, 124304.
- Zhang, J., Lang, H.P., et al., 2006. *Nat. Nanotechnol.* 1, 214–220.
- Ziegler, C., 2004. *Anal. Bioanal. Chem.* 379, 946–959.